5

Control Analysis and Feedback Techniques for Multi Agent Robots

Salman Ahmed[1] and Mohd Noh Karsiti[2] and Robert N. K. Loh[3]
[1,2]*Electrical & Electronic Engineering, Universiti Teknologi PETRONAS*
[3]*Electrical and Computer Engineering, Oakland University,*
[1,2]*Malaysia*
[3]*United States*

1. Introduction

Multi agent robots involve a team of robots working together socially to achieve a task. Collaboration among agents is motivated by a need to complete complex tasks that require more capabilities than a single robot can provide. Applications of multi agent robots can be found in the fields of underwater robotics, air traffic control, intelligent highways, security patrols, tele-surgery and mines and ores detection (Bichhi & Pallottino, 2000; Ferber, 1999; Parker, 1994). The accuracy of task completion by multi agent robots depends on the control strategies implemented in the robots to minimize the effect of external disturbances and errors. Multi agent unicycle robots can be represented as an underactuated system in which the number of control inputs is less than the number of states. In such a system, the controllable degrees of freedom are less than the total degrees of freedom. Hence, the motion control problems for underactuated systems are of particular interest for research (Kolmanovsky & McClamroch, 1995).

1.1 Motion planning

Motion planning for multi agent robots involves the following basic motion tasks (Luca et. al. 2000).

Point to point motion: In point to point motion, the multi agent robots must reach a final goal starting from a given initial configuration. The trajectory or path for the multi agent robots is not specified in advance.

Trajectory tracking: In trajectory tracking, the multi agent robots must reach a final configuration following a certain desired trajectory in the cartesian space. The desired trajectory is a function of time.

In terms of control systems, point to point motion can be compared with a regulation control for an equilibrium point in the state space. Trajectory tracking can be compared with a tracking problem such as to minimize the error between the reference and desired trajectory to zero.

1.2 Feedback control techniques

In automatic control systems, feedback improves the system performance by completing the task even if external disturbances and initial errors are present. Hence, the effect of

Source: Multiagent Systems, Book edited by: Salman Ahmed and Mohd Noh Karsiti,
ISBN 978-3-902613-51-6, pp. 426, February 2009, I-Tech, Vienna, Austria

unmodeled events at running time, such as slipping of wheels or wrong initial localization, is minimized. Furthermore, feedback control techniques can be used to stabilize the system. There are various feedback control design techniques available for feedback control, some of which are listed as follows (Nise, 2004; Khalil, 2002; Slotine & Li, 1991).

- Root locus method
- PID method
- Poles placement
- Cascaded systems theory
- Linearization of corresponding error model
- Approximate linearization
- Feedback linearization

The design of nonlinear feedback control strategies is a challenging task. A common practice is to linearize the system. After linearizing the model of multi agent robotic system, feedback control strategies can be designed for trajectory tracking and point to point motion.

1.3 Formation control strategies

The control of multi agent robotic system requires coordination at different levels. At the lowest level, it is necessary for each robot to control its motion and to avoid collisions with its neighbors. Furthermore, the robotic agent should move along a desired trajectory. At an immediate supervisory level, it is necessary to maintain a certain formation strategy.

The various approaches to formation control can be divided roughly into three categories: behavior-based, virtual structure formation and leader-follower formation (Tabuada, et al., 2005). The behavior-based formation is a distributed approach (Balch & Arkin, 1998), while the virtual structure formation is a centralized approach (Tan & Lewis, 1997). Majority of the current algorithms that focus on behavior-based or virtual structure formation are implemented on robots having visual capabilities (Langer et al., 1994; Clark, 2004). Similarly, behavior-based formation focuses on peer to peer communication, whereas in this paper Bluetooth is considered, which acts in a master-slave fashion (Morrow, 2002). Therefore, leader-follower formation is the best available formation control and it is used as a formation control strategy for the multi agent nonholonomic robots (Desai, 1998).

In the leader-follower formation, one of the agent robots is designated as the leader and the others as followers. The leader agent plans and follows a desired trajectory. The follower agents follow the leader agent with a desired distance and separation bearing angle. The leader agent is responsible for guiding the formation.

There has been considerable research in designing feedback linearized strategies for trajectory tracking of multi agent robots. However, most of the feedback linearized strategies are designed either for a single robot (Oriolo, 2002) or for the follower robots using the leader-follower formation (Desai, 1998). Similarly, there have been feedback linearized strategies for vision-based multi agent robots (Das, 2002). In this chapter, the multi agent robots have communication abilities only. The principal investigation of this chapter is to present a comparative analysis of different feedback control strategies for multi agent robots having communication abilities. The comparative analysis is presented for trajectory tracking as well as posture stabilization of the multi agent robots. In this chapter, a development framework for simulation and implementation based on communication abilities is also presented for multi agent robots.

2. Kinematic model of leader-follower formation

A multi agent robot system can be described by its state, X, which is a composition of the individual robots states as

$$X = \left[x_1, x_2, \ldots, x_n\right]^T \quad , \quad \dot{X} = F(X,t) \tag{1}$$

The state of each robot varies as a function of its continuous state, x, and the input vector, u. Also each robot receives information about the rest of the system, z. The input vector, u, depends on the discrete state of the robot, h, which can be either the leader, l, or follower, f, state. The state equations of each robot, $i = l, f$, can be expressed as

$$\dot{x}_i = f_{i,h}(x_i, u_i, \hat{z}_i) \tag{2}$$

To model the kinematics of the leader robot, l, in the 2D plane, the configuration $p_l = [x_l, y_l, \theta_l]^T$ (with respect to the global frame (X_G, Y_G) in Fig. 1) is used. This configuration of the robot stands for three degrees of freedom. Let the control inputs for the leader robot be denoted by v_l and ω_l. The equations for the leader robot can be written as

$$\begin{pmatrix} \dot{x}_l \\ \dot{y}_l \\ \dot{\theta}_l \end{pmatrix} = \begin{pmatrix} \cos\theta_l \\ \sin\theta_l \\ 0 \end{pmatrix} v_l + \begin{pmatrix} 0 \\ 0 \\ 1 \end{pmatrix} \omega_l \tag{3}$$

The wheels in the model of Eq. 3 are assumed not to slip and exhibit purely rolling motion. The same constraint is observed for the follower robots, f. The nonholonomic constraint is expressed as

$$-\dot{x}_i \sin\theta_i + \dot{y}_i \cos\theta_i = 0 \tag{4}$$

The follower robots are modeled relatively to the leader robot. The modeling of the follower robots depend on the formation controllers, which are discussed as follows.

2.1 Separation-bearing controller (SBC)

The separation bearing controller is used for two robots. The follower robot follows the leader while maintaining a desired relative distance and separation bearing angle with respect to the leader robot. Such type of leader-follower formation control strategy is also denoted by l–φ control strategy. A schematic for this control strategy is shown in Fig. 1.

Let φ_{lf} denote the separation bearing angle between the leader and follower robot. The separation distance between the center of axis between the rear wheels of the leader, and the front castor of the follower robot is denoted by l_{lf}. The position coordinates for the front castor of the follower robot is represented by (x, y). The distance between the front castor and the center of axis between the rear wheels for each robot is denoted by d. Let (x_l, y_l) represent the mid point on the axis between the rear wheels. The leader robot position is expressed by $p_l = [x_l, y_l, \theta_l]^T$ and the control inputs by $u_l = [v_l, \omega_l]^T$.. The follower robot position is represented by $p_f = [x_f, y_f, \theta_f]^T$ and the control inputs by $u_f = [v_f, \omega_f]^T$.

Knowing the leader robot position and the separation distance, the follower robot position can be calculated as follows.

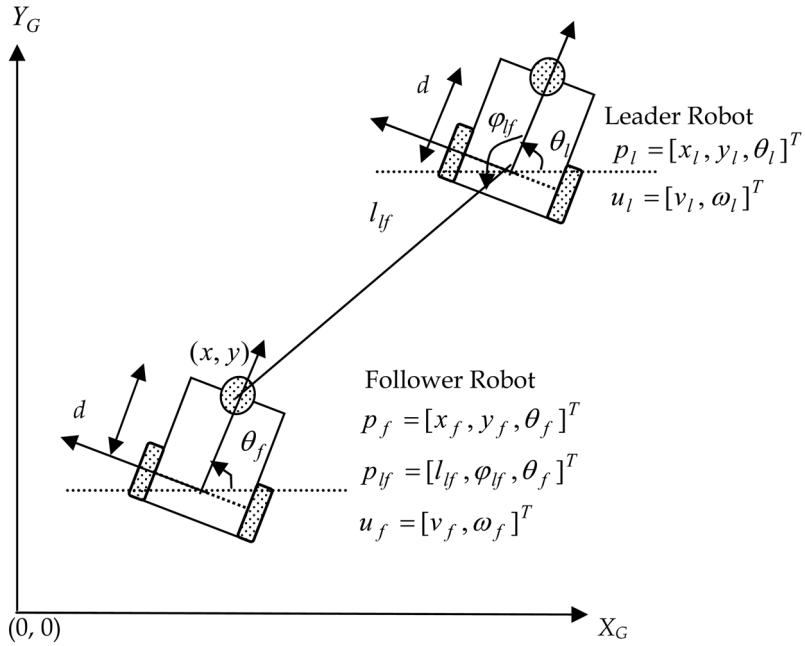

Fig. 1. Leader-follower formation using separation-bearing controller.

$$\begin{aligned} x_f &= x + d\cos\theta_f \\ y_f &= y + d\sin\theta_f \end{aligned} \tag{5}$$

where d is the distance between the mid point of the axis between rear wheel and the front castor wheel. The follower robot is modeled relatively to the leader robot as $p_{lf} = [l_{lf},\ \varphi_{lf},\ \theta_f]^T$. The new state vector, p_{lf}, can be expressed as given by Eq. (6).

$$\begin{aligned} l_{lf} &= \sqrt{(x_l - x_f - d\cos\theta_f)^2 + (y_l - y_f - d\sin\theta_f)^2} \\ \varphi_{lf} &= \pi - \arctan 2(y_f + d\sin\theta_f - y_l, x_l - x_f - d\cos\theta_f) - \theta_l \end{aligned} \tag{6}$$

Differentiating Eq. (6) and combining with Eq. (4), the kinematic model for the follower robot is obtained as

$$\begin{aligned} \dot{l}_{lf} &= v_f\cos\gamma - v_l\cos\varphi_{lf} + d\omega_f\sin\gamma \\ \dot{\varphi}_{lf} &= \frac{v_l\sin\varphi_{lf} - v_f\sin\gamma - \omega_l l_{lf} + d\omega_f\cos\gamma}{l_{lf}} \\ \dot{\theta}_f &= \omega_f \end{aligned} \tag{7}$$

where $\gamma = \theta_l - \theta_f + \varphi_{lf}$. In order to avoid collision between the leader and the follower robots, a requirement that $l_{lf} > 2d$ must be ensured.

2.2 Separation-separation controller (SSC)

This controller is used when multiple robots are present in the formation. Such type of control strategy is also denoted by *l*–*l*. A schematic for this control strategy is shown in Fig. 2. In the *l* – *l* formation strategy, the leader robot 2 is actually a follower relative to leader robot 1. The leader robot 2 can be modeled using *l*–*φ* controller. The follower robot can be expressed relative to the leader robot 1 and 2 as $p_f = [l_{1f}, l_{2f}, \theta_f]^T$. In the *l* – *l* control strategy, the aim is to maintain the desired lengths l_{1f}^d and l_{2f}^d with respect to both leader robots. Again, to avoid collision $l_{1f} > 2d$ and $l_{2f} > 2d$ must be ensured. The separation distances for the leader robots can be expressed as

$$\begin{aligned} l_{1f} &= \sqrt{(x_1 - x_f - d\cos\theta_f)^2 + (y_1 - y_f - d\sin\theta_f)^2} \\ l_{2f} &= \sqrt{(x_2 - x_f - d\cos\theta_f)^2 + (y_2 - y_f - d\sin\theta_f)^2} \end{aligned} \tag{8}$$

Differentiating Eq. (8), the kinematic model for the follower robot is obtained as

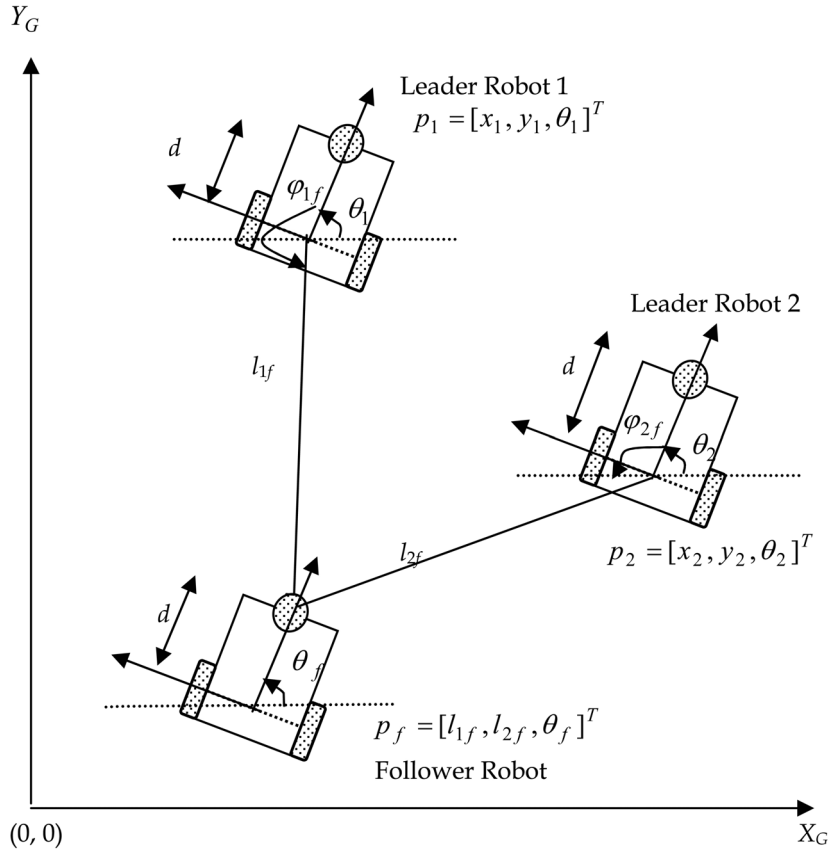

Fig. 2. Leader-follower formation using separation-separation controller.

$$\begin{aligned} \dot{l}_{1f} &= v_f \cos\gamma_1 - v_1 \cos\varphi_{1f} + d\omega_f \sin\gamma_1 \\ \dot{l}_{2f} &= v_f \cos\gamma_2 - v_2 \cos\varphi_{2f} + d\omega_f \sin\gamma_2 \\ \dot{\theta}_f &= \omega_f \end{aligned} \tag{9}$$

where $\gamma_1 = \theta_1 - \theta_f + \varphi_{1f}$ and $\gamma_2 = \theta_2 - \theta_f + \varphi_{2f}$.

3. Development framework for multi agent robots

3.1 Simulation platform

The simulation platform is implemented using MATLAB/Simulink. For simulation, Bluetooth USB dongles are used. Each dongle is connected to a computer. These dongles are configured to form a Bluetooth piconet. A MATLAB/Simulink session runs on each computer, which communicates with other sessions in the piconet. Each session models the leader-follower formation for the leader and follower robots. The master device in the piconet acts as the leader robot and the slaves act as follower robots. This simulation platform for the leader and follower robots is shown in Figs. 3 and 4, respectively.

For a desired and feasible goal trajectory, $[x_d(t), y_d(t)]^T$, the feedforward controller generates the feedforward control inputs, $[v_d, \omega_d]^T$, for the leader robot. Using the leader-follower strategy, the leader robot transmits its own control inputs to the follower robots. The control inputs are transmitted using the Bluetooth piconet. The follower robots receive the leader robot inputs and derive their own control inputs, $[v_f, \omega_f]^T$, using the leader-follower formation control and the information sent by the leader robot. The control inputs for both the leader and follower robots are fed into the feedback strategies. The feedback control strategies generate the actual inputs based on the feedforward inputs and feedback states of the robots.

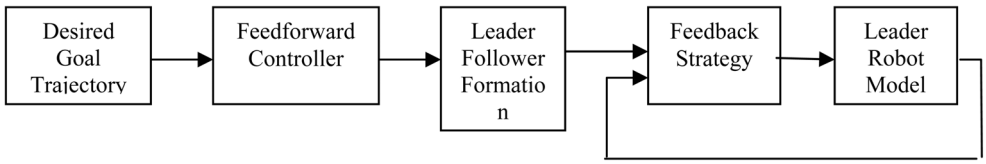

Fig. 3. Framework for the leader robot

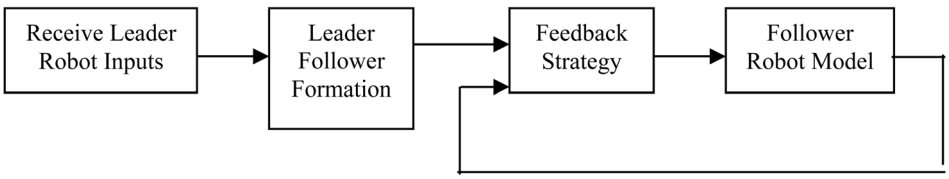

Fig. 4. Framework for the follower robot

3.2 Bluetooth library development

The Bluetooth protocol suite is implemented in software as well as in hardware device. The software protocol suite for Bluetooth piconet supports three modes of operation which includes Personal Area Network User, PANU, Group Adhoc Network, GN, and Network

Access Point, NAP. In this paper, the multi agent robots communicate using the GN mode. The message format used for communication conforms to the standard Agent Control Language, ACL, provided by Foundation for Intelligent Physical Agents (FIPA, 2002).
Currently, the TCPIP toolbox available in MATLAB does not provide support for TCP connections between two computers. Rather the TCPIP toolbox provides functions that can be used to acquire data from a network device such as an oscilloscope. So to overcome this limitation, a shared library was developed using Windows Socket programming (Rydesater, 2007). This shared library was then accessed in MATLAB to communicate with other MATLAB sessions in the Bluetooth piconet.

3.3 Feedforward controller

Assuming that the leader robot follows a desired cartesian trajectory $[x_d(t),\ y_d(t)]^T$ with $t \in [0, T]$. The flat outputs for the leader robot system are $[x_l(t),\ y_l(t)]^T$ (Luca et al., 2001). The flat outputs for a system are helpful in a way that all the system inputs, states and outputs can be determined algebraically from the flat outputs without integration. The desired orientation angle for the leader robot, θ_d, can be calculated as

$$\theta_d = \text{atan2}\,(\dot{y}_d, \dot{x}_d) \tag{10}$$

where atan2 is the fourth-quadrant inverse tangent and is undefined only if both arguments are zero. Assuming v_d and ω_d are the desired velocities for the leader robot, whereas the actual velocities are denoted by v and ω. Differentiating Eq. (3) with respect to time, the feedforward control inputs for the leader robot are computed as

$$v_d(t) = \pm\sqrt{\dot{x}_d^2(t) + \dot{y}_d^2(t)} \tag{11}$$

$$w_d(t) = \frac{\ddot{y}_d(t)\dot{x}_d(t) - \ddot{x}_d(t)\dot{y}_d(t)}{\dot{x}_d^2(t) + \dot{y}_d^2(t)} \tag{12}$$

The sign for $v_d(t)$ will determine the forward or backward motion of the robots. Eq. (12) is not defined when $v_d(t)$ is equal to zero.

4. Posture stabilization control strategies

The objective of posture stabilization controller is to reach a final desired configuration starting from an initial point, without the need to plan a trajectory. The available techniques are to use smooth time-varying feedback, non smooth time-varying feedback and design based on polar coordinates. All of these control strategies are discussed as follows.

4.1 Smooth time-varying feedback controller

The smooth time-varying feedback controller for posture stabilization was first presented in (Wit et al., 1994). Let the desired position for the leader robot be $p_d = [x_d,\ y_d,\ \theta_d]^T$, whereas the actual position is denoted by $p_l = [x_l,\ y_l,\ \theta_l]^T$. The error between the desired and actual position is expressed as

$$e = \begin{bmatrix} e_1 \\ e_2 \\ e_3 \end{bmatrix} = \begin{bmatrix} \cos\theta_l & \sin\theta_l & 0 \\ -\sin\theta_l & \cos\theta_l & 0 \\ 0 & 0 & 1 \end{bmatrix} \begin{bmatrix} x_d - x_l \\ y_d - y_l \\ \theta_d - \theta_l \end{bmatrix} \tag{13}$$

The feedback strategy using the smooth time-varying feedback controller is given as

$$\begin{aligned} u_1 &= -k_1(v_d(t), \omega_d(t))e_1, \\ u_2 &= -k_2 v_d(t)\frac{\sin e_3}{e_3} e_2 - k_3(v_d(t), \omega_d(t))e_3 \end{aligned} \tag{14}$$

where k_1, k_2 and k_3 are feedback gains, and. The feedback gains are expressed as

$$\begin{aligned} &k_1(v_d(t), \omega_d(t)) = k_3(v_d(t), \omega_d(t)) = 2\zeta a = 2\zeta\sqrt{w_d^2(t) + b v_d^2(t)} \\ &k_2 = b|v_d(t)| \end{aligned} \tag{15}$$

where b is a positive constant. For generating the actual control inputs, Eq. (16) is used.

$$\begin{aligned} v &= v_d \cos(\theta_d - \theta_l) + k_1(v_d(t), \omega_d(t))[\cos\theta(x_d - x_l) + \sin\theta(y_d - y_l)] \\ \omega &= \omega_d + k_4 v_d \frac{\sin(\theta_d - \theta_l)}{\theta_d - \theta_l}[\cos\theta(y_d - y_l) - \sin\theta(x_d - x_l)] + k_3(v_d, \omega_d)(\theta_d - \theta_l). \end{aligned} \tag{16}$$

The feedback control law expressed by Eq. (16) globally asymptotically stabilizes the origin at $e = 0$, which is demonstrated using Lyapunov stability theory.

4.2 Design based on polar coordinates

The control law for posture stabilization based on the polar coordinates was presented in (Aicardi et al., 1995; Luca et al., 2001). This control design is based on the change of original coordinates to polar coordinates. Let ψ be the distance of the reference point (x_l, y_l) of the leader robot from the goal, μ be the angle of the pointing vector to the goal with respect to the robot main axis and ϕ be the angle of the same pointing vector with respect to the x-axis of the robot. The state transformation is given as

$$\begin{aligned} \psi &= \sqrt{x^2 + y^2} \\ \mu &= \tan^{-1}(y/x) - \theta + \pi \\ \phi &= \mu + \theta \end{aligned} \tag{17}$$

Differentiating Eq. (17), the transformed kinematic equations can be written as

$$\begin{aligned} \dot{\psi} &= -v\cos\mu \\ \dot{\mu} &= \frac{\sin\mu}{\psi} v - \omega \\ \dot{\phi} &= v\frac{\sin\mu}{\psi} \end{aligned} \tag{18}$$

The feedback control law based on polar coordinates is given as follows

$$v = k_1 \psi \cos \mu$$
$$\omega = k_2 \mu + k_1 \frac{\sin \mu \cos \mu}{\mu} (\mu + k_3 \phi) \tag{19}$$

The feedback law of Eq. (19) globally asymptotically stabilizes the system.

4.3 Dynamic feedback linearized controller

The dynamic feedback linearized controller was presented in (Luca et al., 2000) The feedback control law is given as

$$r_1 = -k_{p1}(x) - k_{d1}(\dot{x})$$
$$r_2 = -k_{p2}(y) - k_{d2}(\dot{y}) \tag{20}$$

where k_{p1}, k_{p2}, k_{d1}, k_{d2} are the feedback gains. The feedback law of Eq. (20) yields exponential convergence from any initial configuration to the origin

5. Trajectory tracking control strategies for the leader robot

In order to track the correct goal trajectory, the feedforward controller generates the velocity inputs. The inputs commands are generated for the leader robot and transmitted to the follower robots using Bluetooth. The kinematics of the leader and the follower robots is modeled using Simulink. Different feedback control strategies are chosen from the literature based on their properties which are briefly discussed below.

Feedback control strategies are designed for the leader as well as follower robots. For the leader robot, the feedback control strategies involve designing strategies for point stabilization and trajectory tracking. For the follower robots, it involves designing strategies for trajectory tracking only. The feedback control strategies are presented as follows.

5.1 Feedback strategy based on approximate linearization

The control objective of feedback controller is to drive the errors $[x_d - x, y_d - y, \theta_d - \theta]^T$ to zero. Linearizing the error dynamics about the equilibrium point, $e = 0$ and $u = 0$, the feedback strategy is expressed as follows (Oriolo et al.,2002).

$$v = v_d \cos(\theta_d - \theta_l) + k_1[\cos\theta(x_d - x_l) + \sin\theta(y_d - y_l)]$$
$$\omega = \omega_d + k_2 \text{sign}(v_d)[\cos\theta(y_d - y_l) - \sin\theta(x_d - x_l)] + \quad k_3(\theta_d - \theta_l) \tag{21}$$

The feedback control strategy of Eq. (21) results in a time-varying system. This means that if the eigenvalues are constant and with negative real part, asymptotic stability is not guaranteed because the system is still time-varying.

5.2 Feedback strategy using cascaded systems theory

This controller was proposed in (Lefeber et al., 2001). The control law is given by Eq. (22)

$$v = v_d + c_2 e_1 - c_3 \omega_d e_2, \qquad c_2 > 0, c_3 > -1$$
$$\omega = \omega_d + c_1 e_3, \qquad c_1 > 0 \tag{22}$$

The control law of Eq. (22) is K–exponentially stable if v_d is bounded and ω_d is persistently exciting. A small modification to this law was also proposed, which is

$$\begin{aligned} v &= v_d + c_2 e_1 - c_3 \omega_d e_2, \qquad c_2 > 0, c_3 > -1 \\ \omega &= \omega_d + c_1 \sin e_3, \qquad c_1 > 0 \end{aligned} \tag{23}$$

The feedback control strategy of Eq. (23) results in local uniform exponential stable system if v_d is bounded and ω_d is persistently exciting.

5.3 Feedback strategy based on linearization of error model

This control strategy was presented in (Kanayama et al., 1991). The control law is given as

$$\begin{aligned} v &= v_d \cos e_3 + K_x e_1, \qquad K_x > 0 \\ \omega &= \omega_d + v_d (K_y e_2 + K_\theta \sin e_3), \quad K_y > 0, K_\theta > 0 \end{aligned} \tag{24}$$

The stability analysis of the control law expressed in Eq. (24) states that if $v_d > 0$, then the system is locally asymptotically stable. Furthermore, if v_d and ω_d are both continuous, v_d, ω_d, K_x, K_θ are all bounded and if $\dot{v}_d$ and $\dot{\omega}_d$ are both sufficiently small, then the system is locally uniformly asymptotically stable.

5.4 Feedback strategy based on full state linearized via dynamic feedback

This feedback strategy was proposed in (Oriolo et al., 2002). The dynamic state feedback compensator is given as

$$\begin{aligned} v &= a(q, \xi) + b(q, \xi) r \\ \dot{\xi} &= c(q, \xi) + d(q, \xi) r \end{aligned} \tag{25}$$

where $\xi(t) \in \Re^v$ is the compensator state vector of dimensions v, and $r(t) \in \Re^v$ is the auxiliary input. For the system modeled by Eq. (3), the output is defined as

$$z = \begin{bmatrix} x \\ y \end{bmatrix}, \quad \dot{z} = \begin{bmatrix} \cos\theta & 0 \\ \sin\theta & 0 \end{bmatrix} \begin{bmatrix} v \\ \omega \end{bmatrix} \tag{26}$$

From Eq. (26), it can be observed that only v affects $\dot{z}$, while ω cannot be recovered. In order to proceed, an integrator, ξ, is added on the linear velocity input v, as

$$\xi = v, \quad \dot{\xi} = a \tag{27}$$

where a is the new input representing the linear acceleration of the leader robot. In terms of ξ, Eq. (26) can be expressed as

$$\dot{z} = \begin{bmatrix} \cos\theta & 0 \\ \sin\theta & 0 \end{bmatrix} \begin{bmatrix} \xi \\ \omega \end{bmatrix} \Rightarrow \dot{z} = \xi \begin{bmatrix} \cos\theta \\ \sin\theta \end{bmatrix} \tag{28}$$

Differentiating Eq. (27), the following is obtained

$$\ddot{z} = \dot{\xi}\begin{bmatrix}\cos\theta \\ \sin\theta\end{bmatrix} + \xi\begin{bmatrix}-\sin\theta \\ \cos\theta\end{bmatrix}\dot{\theta} \tag{29}$$

Substituting the value of $\dot{\xi}$ from Eq. (27) and $\dot{\theta} = \omega$, the following is obtained

$$\ddot{z} = a\begin{bmatrix}\cos\theta \\ \sin\theta\end{bmatrix} + \xi\begin{bmatrix}-\sin\theta \\ \cos\theta\end{bmatrix}\omega = \begin{bmatrix}\cos\theta & -\xi\sin\theta \\ \sin\theta & \xi\cos\theta\end{bmatrix}\begin{bmatrix}a \\ \omega\end{bmatrix} \tag{30}$$

From Eq. (30), it can be observed that the decoupling matrix multiplied with the modified input (a, ω) is nonsingular provided that $\xi \neq 0$. Let $\ddot{z} = r$, so the inputs can be obtained as

$$\begin{bmatrix}a \\ \omega\end{bmatrix} = \begin{bmatrix}\cos\theta & -\xi\sin\theta \\ \sin\theta & \xi\cos\theta\end{bmatrix}^{-1}\begin{bmatrix}r_1 \\ r_2\end{bmatrix} = \begin{bmatrix}\cos\theta & \sin\theta \\ -\sin\theta/\xi & \cos\theta/\xi\end{bmatrix}\begin{bmatrix}r_1 \\ r_2\end{bmatrix} \tag{31}$$

Substituting the values for original inputs, the resulting dynamic compensator and the inputs are

$$\begin{aligned} v &= \xi \\ \omega &= \frac{r_2\cos\theta - r_1\sin\theta}{\xi} \\ \dot{\xi} &= r_1\cos\theta + r_2\sin\theta \end{aligned} \tag{32}$$

As one integrator, ξ, was added, hence the order of the dynamic compensator is one. The new coordinates can be written as

$$\begin{aligned} z_1 &= x \\ z_2 &= y \\ z_3 &= \dot{x} = \xi\cos\theta \\ z_4 &= \dot{y} = \xi\sin\theta \end{aligned} \tag{33}$$

The extended system of Eq. (33) is fully linearized in a controllable form. The decoupled chain of input output integrators can be written as

$$\begin{aligned} \ddot{z}_1 &= r_1 \\ \ddot{z}_2 &= r_2 \end{aligned} \tag{34}$$

Assuming that the robot must follow a smooth output trajectory $[x_d(t), y_d(t)]^T$. The globally exponentially stabilizing feedback law for the trajectory is given as

$$\begin{aligned} r_1 &= \ddot{x}_d(t) + k_{p1}(x_d(t) - x) + k_{d1}(\dot{x}_d(t) - \dot{x}) \\ r_2 &= \ddot{y}_d(t) + k_{p2}(y_d(t) - y) + k_{d2}(\dot{y}_d(t) - \dot{y}) \end{aligned} \tag{35}$$

with PD gains chosen as $k_{pi} > 0$, $k_{di} > 0$, for $i = 1,2$. The values of $\dot{x}$ and $\dot{y}$ can be computed from Eq. (33) as a function of the robot state and the compensator state, ξ. The values of the feedback gains are chosen such that the polynomial expressed by Eq. (36) is Hurwitz.

$$\lambda^2 + k_{di}\lambda + k_{pi}, \quad i = 1,2 \tag{36}$$

6. Feedback strategies for the follower robots

In this section, the feedback strategies for the follower robots are presented. The follower robots follow the leader robot with a desired distance and angle. The feedback laws as presented for both of the formation control strategies.

6.1 Feedback strategy for separation bearing controller

The kinematic model for the follower robot using the separation bearing controller was expressed in Eq. (7). The kinematic model can be written in compact form as given as

$$\begin{aligned} \dot{z}_{lf} &= G_{\mathrm{SB}}(z_{lf}, \gamma)u_f + F_{\mathrm{SB}}(z_{lf})u_l \\ \dot{\theta}_f &= \omega_f \end{aligned} \tag{37}$$

where $z_{lf} = (l_{lf}, \varphi_{lf})$, $u_f = (v_f, \omega_f)$, $u_l = (v_l, \omega_l)$ and

$$\begin{aligned} G_{\mathrm{SB}} &= \begin{bmatrix} \cos\gamma & d\sin\gamma \\ \dfrac{-\sin\gamma}{l_{lf}} & \dfrac{d\cos\gamma}{l_{lf}} \end{bmatrix} \\ F_{\mathrm{SB}} &= \begin{bmatrix} -\cos\varphi_{lf} & 0 \\ \sin\varphi_{lf}/l_{lf} & -1 \end{bmatrix} \end{aligned} \tag{38}$$

The input-output linearization technique begins by defining the output as $z_{lf} = (l_{lf}, \varphi_{lf})$ (Desai, 1998). Differentiating the output, Eq. (39) is obtained.

$$\dot{z}_{lf} = G_{\mathrm{SB}}(z_{lf}, \gamma)u_f + F_{\mathrm{SB}}(z_{lf})u_l = A(z_{lf})u_f + B \tag{39}$$

The determinant of the decoupling matrix, $A(z_{lf})$, is $d/l \neq 0$. Since $A(z_{lf})$ is nonsingular, the control velocities for the follower robot can be expressed as

$$u_f = G_{\mathrm{SB}}^{-1}(p_{\mathrm{SB}} - F_{\mathrm{SB}}u_l) \tag{40}$$

where p_{SB} is an auxiliary control input given as

$$p_{\mathrm{SB}} = K\tilde{z}_{lf} = \begin{bmatrix} k_1 & 0 \\ 0 & k_2 \end{bmatrix} \begin{bmatrix} l_{lf}^d - l_{lf} \\ \varphi_{lf}^d - \varphi_{lf} \end{bmatrix} \tag{41}$$

with $k_1, k_2 > 0$ as the controller gains. The control inputs for the follower robot are expressed as

$$v_f = \rho - d\omega_f \tan\gamma$$

$$\omega_f = \frac{\cos\gamma}{d}\{k_a l_{lf}(\varphi_{lf}^d - \varphi_{lf}) - v_l \sin\varphi_{lf} + l_{lf}\omega_l + \rho\sin\gamma\}$$

where (42)

$$\rho = \frac{k_b(l_{lf}^d - l_{lf}) + v_l\cos\varphi_{lf}}{\cos\gamma}$$

$$\gamma = \varphi_{lf} + \theta_l - \theta_f$$

The stability of the controller expressed by Eq. (42) was presented in (Desai, 1998; Desai et. al., 1998). If the linear velocity of the leader robot is lower bounded *i.e.* $v_l > 0$, angular velocity is bounded *i.e.* $\omega_l < \omega_{max}$, and the initial orientation is such that $|\theta_l(0) - \theta_f(0)| < \pi$, then the system of Eq. (42) is stable and the output error converges to zero exponentially.

6.2 Feedback strategy for separation-separation controller

Using input-output linearization techniques the control law for the follower robot is given as

$$v_f = \frac{k_1(l_{1f}^d - l_{lf}) + v_1\cos\varphi_{1f} - d\omega_f\sin\gamma_1}{\cos\gamma_1}$$

$$\omega_f = \frac{k_1(l_{1f}^d - l_{lf})\cos\gamma_2 + v_1\cos\varphi_{1f}\cos\gamma_2}{d\sin(\gamma_1 - \gamma_2)} + \frac{v_2\cos\varphi_{2f}\cos\gamma_1 - k_2(l_{2f}^d - l_{2f})\cos\gamma_1}{d\sin(\gamma_1 - \gamma_2)} \quad (43)$$

where

$$\gamma_i = \varphi_{if} + \theta_i - \theta_f, \qquad i = 1,2$$

The stability analysis of the feedback control strategy expressed in Eq. (43) was presented in (Desai, 1998; Desai et al., 1998). Assuming the linear velocity of the leader robot 1 is lower bounded *i.e.* $v_1 > 0$, angular velocity is bounded *i.e.* $\omega_1 < \omega_{max}$, and the relative orientation between the robots is such that $|\theta_l(0) - \theta_i(0)| < \pi$ with $i = 2, f$. If the control input u_{2f} is obtained using feedback linearization, then the system of Eq. (43) is stable and the output converges exponentially to the desired value z_d.

7. Simulation results

The above stated feedback laws for posture stabilization and trajectory tracking were simulated using MATLAB/Simulink. The multi agent robot system using leader-follower formation was modeled in MATLAB/Simulink. The results of simulation are summarized as follows.

7.1 Trajectory tracking controllers for the leader robot

In the first test, the desired trajectory was defined as follows.

$$x_d(t) = 10\sin(t/20),\ y_d(t) = 10\sin(t/40) \quad (44)$$

The desired trajectory of Eq. (44) begins at the origin (0, 0). The trajectory completes a full cycle when $T = 2\pi$ (40) ≈ 251.3 sec. The actual trajectory and the error norm using full state dynamic feedback linearized controller are shown in Fig. 5. The values for different parameters in the feedback controllers are listed in Table 1. The error statistics for the given trajectory are summarized in Table 2.

Controllers	Parameters values
Feedforward	$v_d(0)= 0.0125\ m/sec$
Approximate linearized feedback	$\zeta = 0.5$, $b = 2$
Cascaded systems feedback	$c_1 = 216.9$, $c_2 = 1.355$ and $c_3 = -0.414$
Linearization of corresponding error model	$K_x = 10$, $K_y = 0.0064$ and $K_\theta = 0.16$
Dynamic linearized feedback	$k_{d1}= k_{d2} =0.7$, $k_{p1}= k_{p2} =1$, $\zeta(0)=v(0)$

Table 1. Parameters values for different feedback controllers

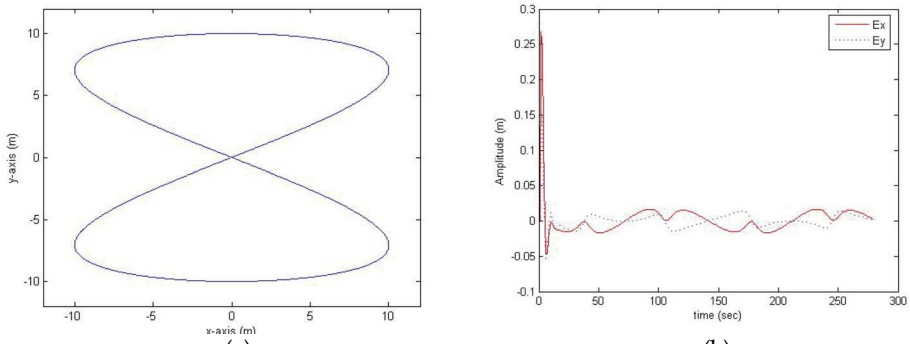

(a) (b)

Fig. 5. (a) Actual trajectory by the leader robot (Eq. 44) using full state dynamic feedback linearized controller (b) Norm of error for trajectory of Eq. (44) using full state dynamic feedback linearized controller

Statistical parameter	Mean (m)	Standard Deviation (m)	Variance (m)
Approximate linearized	0.1622	0.7746	0.6001
Cascaded systems controller	0.5154	0.6758	0.4568
Linearization of corresponding error model	3.3460	2.9895	8.9369
Full state linearized via dynamic feedback	0.0192	0.0410	0.00017

Table 2. Error statistics using different feedback controllers for trajectory of Eq. (44)

In the second series of simulation, the desired trajectory was defined as follows.

$$x_d(t) = t\ ,\ y_d(t) = 10\sin(t) \tag{45}$$

The desired trajectory of Eq. (45) begins at the origin (0, 0) and is a sinusoidal signal. This trajectory is shown in for T = 1000 sec. The same values of Table 1 for the parameters of the feedback controllers were used. Table 3 summarizes the error statistics for the given trajectory using different feedback controllers. The actual trajectory using full state linearized via dynamic feedback controller is shown in Fig. 6. In the third series of simulation, the desired trajectory was defined as follows.

$$x_d(t) = 10\cos(t/20)\,,\; y_d(t) = 10\sin(t/20) \tag{46}$$

The desired trajectory of Eq. (46) begins at the origin (10, 0) and completes a full cycle when $T = 2\pi(20) \approx 125.67$ sec. The leader robot is assumed to be at the origin (0, 0). The actual trajectory for the leader robot using approximate linearized and cascaded systems controller is shown in Fig. 7. The actual trajectory using linearization of corresponding error model and full state linearized via dynamic feedback controller is shown in Fig. 8. Table 4 summarizes the error statistics for the given trajectory using different feedback controllers.

Statistical parameter	Mean (m)	Standard Deviation (m)	Variance (m)
Approximate linearized	0.2808	0.2619	0.0686
Cascaded systems controller	0.6908	0.6538	0.4274
Linearization of corresponding error model	1.0406	0.8041	0.6465
Full state linearized via dynamic feedback	0.2265	0.6846	0.4687

Table 3. Error statistics using different feedback controllers for trajectory of Eq. (45)

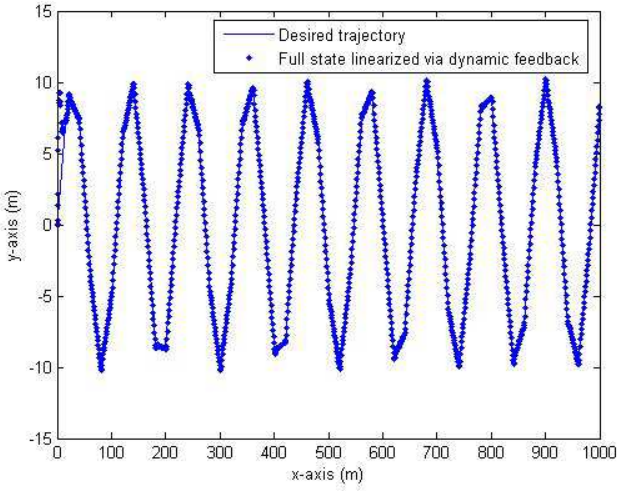

Fig. 6. Actual trajectory for Eq. (45) using full state dynamic feedback linearized controller

Statistical parameter	Mean (m)	Standard Deviation (m)	Variance (m)
Approximate linearized	0.9627	2.4787	6.1438
Cascaded systems controller	9.7688	0.7949	0.6319
Linearization of corresponding error model	11.3544	1.3286	1.7651
Full state linearized via dynamic feedback	1.0957	2.8231	7.9700

Table 4. Error statistics using different feedback controllers for trajectory of Eq. (46)

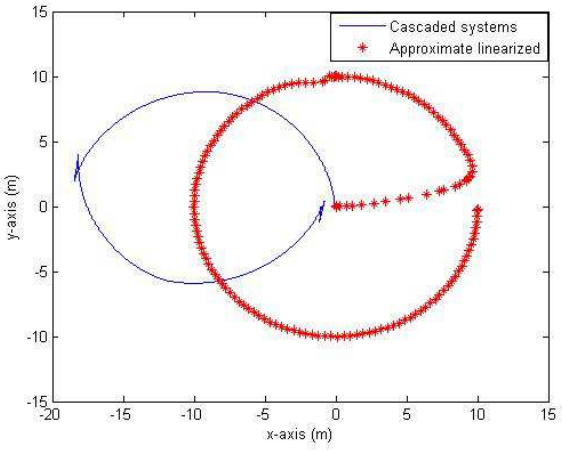

Fig. 7. Actual trajectory for Eq. (46) using approximate linearized and cascaded systems controller

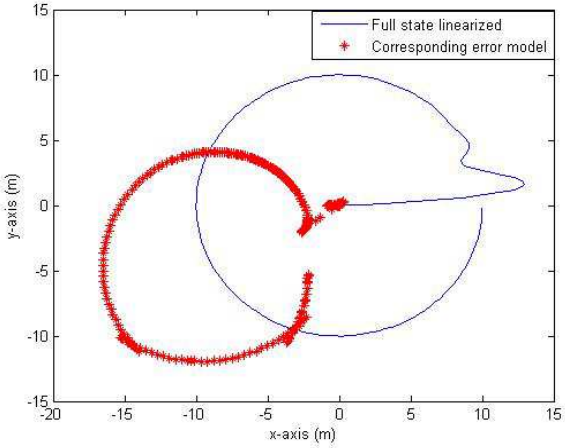

Fig. 8. Actual trajectory for Eq. (46) using linearization of corresponding error model & full state dynamic feedback linearized controller

Based on the above simulation results for the leader robot, it is observed that the full state linearized via dynamic feedback controller minimizes the mean of error more rapidly for the given trajectories. The cascaded systems and linearization of corresponding error model controllers fail to track the correct trajectory of Eq. (46). The reason for failure to track the correct trajectory using cascaded systems controller is that one of the conditions for stability using cascaded systems controller is that ω_d should be persistently exciting. As in trajectory of Eq. (46), ω_d is not persistently exciting, so the controller can not correctly track the desired trajectory. Using the controller based on linearization of corresponding error model, the system is stable provided $\dot{\omega}_d$ is sufficiently small, which is not the case here. Therefore, the cascaded systems controller and controller based on linearization of corresponding error model fail to track the desired trajectory of Eq. (46). Therefore, it can be concluded for the leader robot, that the full state linearized via dynamic feedback is the preferred control strategy for the given trajectories.

7.2 Trajectory tracking controllers for the follower robots

For the follower robots using the separation bearing controller, the following parameters were considered.

$$\begin{aligned} l_{lf}^{d} &= 2 \\ \varphi_{lf}^{d} &= \pi/3 \\ k_1 &= k_2 = 1 \\ d &= 1 \end{aligned} \tag{47}$$

The trajectory of Eq. (44) (eight shaped) and Eq. (46) (circular shaped) were used as the desired reference trajectory for the leader robot. The full state linearized via dynamic feedback controller was used by the leader robot. The actual trajectories for the leader-follower formation using Eq. (44) and (46) for separation bearing controller are shown in Figs. 9 and 10, respectively.

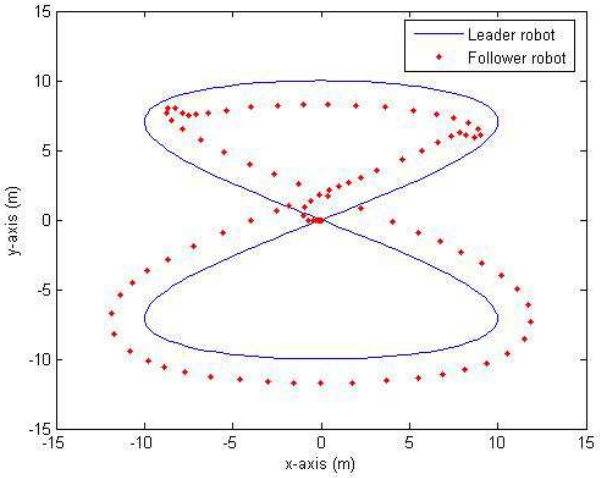

Fig. 9. Actual trajectory using separation bearing controller for Eq. (44)

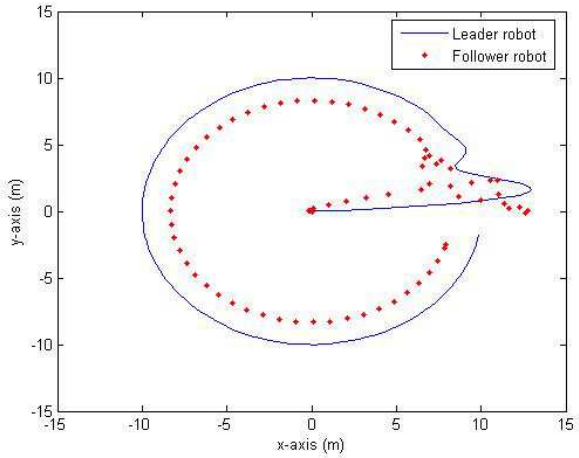

Fig. 10. Actual trajectory using separation bearing controller for Eq. (46)

In another set of simulation, the separation bearing angle was changed as follows.

$$\begin{aligned} \varphi_{lf}^{d} &= \pi/3 \quad \text{for } t < 100 \\ \varphi_{lf}^{d} &= \pi + \pi/3 \quad \text{for } t \geq 100 \end{aligned} \tag{48}$$

The actual trajectory for the leader-follower formation using Eq. (48) is shown in Fig. 11.

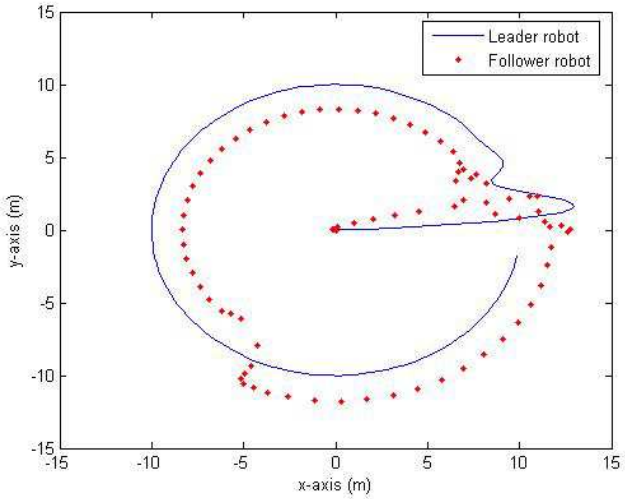

Fig. 11. Actual trajectory using separation bearing controller for Eq. (46)

For the follower robots, using the separation-separation controller, the following parameters were considered.

$$
\begin{aligned}
l_{1f}^{d} &= 2 \\
l_{2f}^{d} &= 2 \\
\varphi_{1f}^{d} &= 3\pi/2 = (240°) \\
\varphi_{2f}^{d} &= 2\pi/3 = (120°) \\
k_1 &= k_2 = 1 \\
d &= 1
\end{aligned}
\tag{49}
$$

The actual trajectory for the leader-follower formation using the trajectory defined by Eq. (44) and (46) for separation-separation controller is shown in Figs. 12 and 13, respectively.

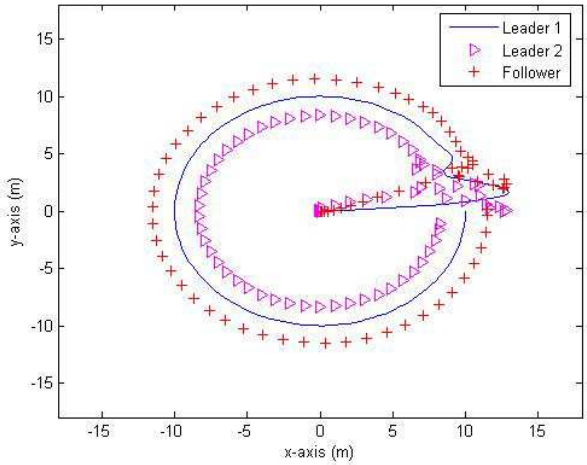

Fig. 12. Actual trajectory using separation-separation controller for Eq. (44)

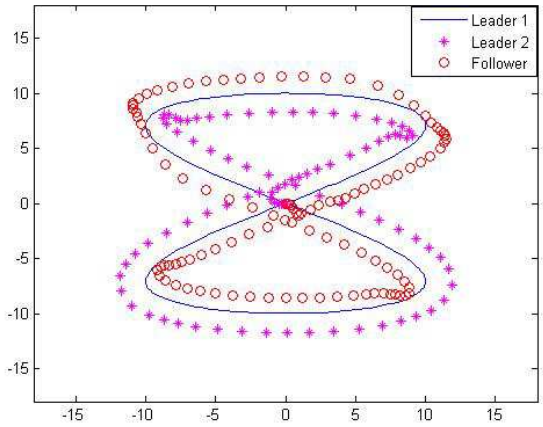

Fig. 13. Actual trajectory using separation-separation controller for Eq. (46)

Based on the simulation results, it is observed that the input-output feedback linearization for the follower robot minimizes the error between the desired and actual formation. Even, if the parameter values of the separation bearing and separation-separation controllers are changed dynamically at run time, the feedback linearized control strategies successfully minimizes the error between the desired and actual trajectory. Hence, the input-output linearized feedback controller is the preferred controller for separation bearing and separation-separation formation control.

7.3 Posture stabilization controllers for the multi agent robots

For posture stabilization, two different goal points were selected as follows. The initial starting position of the leader and follower robots is (-10,-10). The first goal point was defined to reach the origin point (0, 0). The second goal point was to reach the point (-10, 10). The trajectory for the leader robot is not defined. The objective of the leader robot is to move towards the goal point. The goal of the follower robots is to follow the leader robot. The simulation results are provided for the leader robot and finally, using the dynamic feedback linearized controller, the follower robots are also considered. The results of the posture stabilization controllers are as follows.

7.3.1 Smooth time-varying feedback controller

The following parameters were used for the smooth time-varying posture stabilization feedback controller of Eq. (16).

$$\begin{aligned} &y_d(t) = 0 \\ &\theta_d(t) = 0 \\ &\omega_d(t) = 0 \\ &v_d(t) = \dot{x}_d(t) = -k_5 x_d(t) + g(e,t) \end{aligned} \tag{50}$$

where

$$g(e,t) = \frac{\exp(k_6 e_2) - 1}{\exp(k_6 e_2) + 1} \sin t$$

The following values of the gains are used.

$$\begin{aligned} k_1 &= 0.5 \\ k_4 &= 2 \\ k_3 &= 1 \\ k_5 &= 1 \\ k_6 &= 50 \end{aligned} \tag{51}$$

The leader robot is assumed to be at the point (-10, -10). The results of smooth time-varying posture stabilization controller for the first and second goal points are shown in Fig. 14 and 15, respectively.

7.3.2 Polar coordinates feedback controller

The following parameters were used for the polar coordinates posture stabilization controller.

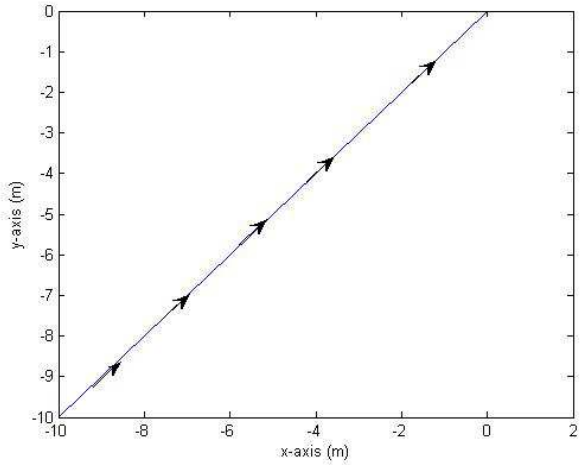

Fig. 14. Actual point to point motion using time-varying feedback controller for the first goal point.

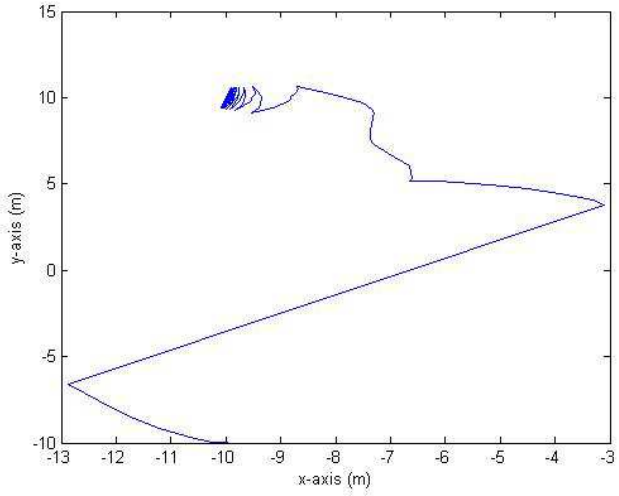

Fig. 15. Actual point to point motion using time-varying feedback controller for the second goal point.

$$k_1 = 1$$
$$k_2 = 3 \tag{52}$$
$$k_3 = 2$$

The robot is assumed to be at the point (-10, -10). The results of point to point motion using this controller for the first and second goal points are shown in Figs. 16 and 17, respectively.

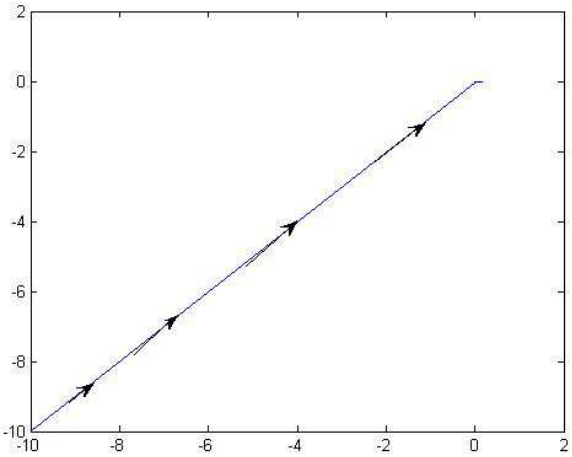

Fig. 16. Actual point to point motion using polar coordinates feedback controller for the first goal point

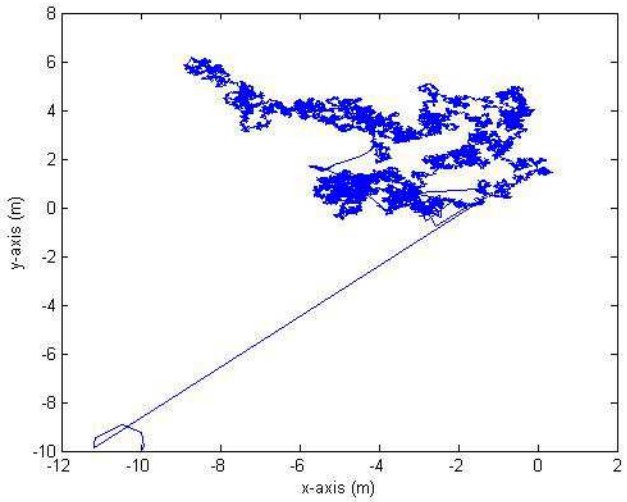

Fig. 17. Actual point to point motion using polar coordinates feedback controller for the second goal point

7.3.3 Full state linearized feedback controller

The following parameters were used for the full state linearized dynamic feedback controller.

$$
\begin{aligned}
k_{p1} &= 2 \\
k_{d1} &= 3 \\
k_{p2} &= 12 \\
k_{d2} &= 7
\end{aligned}
\tag{53}
$$

The robot is assumed to be at the point (-10, -10) and the goal point is origin. The results of point to point motion using this controller for the first and second goal points are shown in Figs. 18 and 19, respectively.

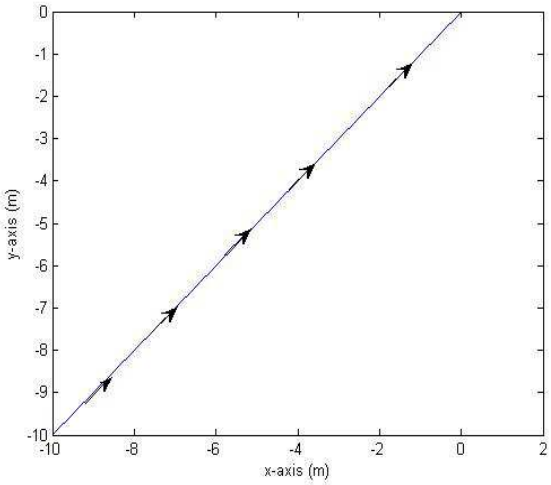

Fig. 18. Actual point to point motion using full state linearized via dynamic feedback controller for the first goal point

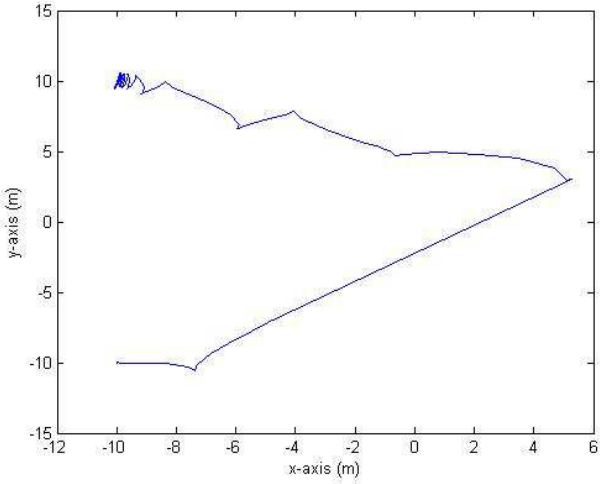

Fig. 19. Actual point to point motion using full state linearized via dynamic feedback controller for the second goal point

Based on the above results, it is found that the posture stabilization feedback controller based on polar coordinates fails to eliminate the error between the desired and the actual goal point. This can be seen in Fig. 19 where the desired goal point is (-10, 10). Although the robot is near to the goal point, still it does not converge to the goal point. The robot achieves the correct goal configuration using the smooth time-varying and dynamic feedback linearized controller. For the follower robots, using SBC the result is shown in Fig. 20.

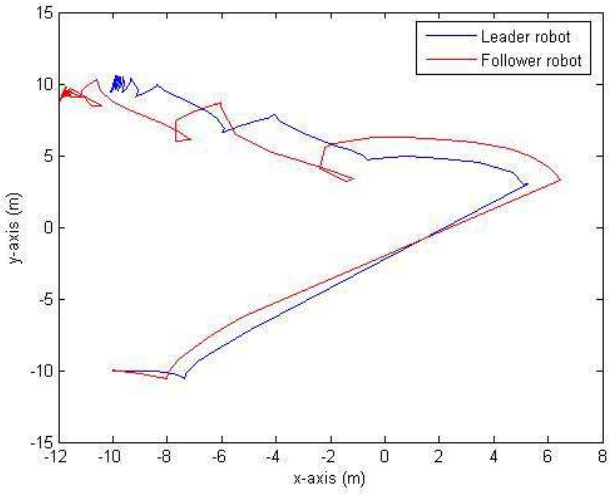

Fig. 20. Actual point to point motion using feedback linearized controllers for SBC formation

8. Conclusions & future work

In this paper, a simulation framework based on the kinematic model for the multi agent robots using the leader-follower formation was presented. The design of feedback controllers for leader-follower formation using feedback linearization techniques was also presented. The follower robots derived their inputs based on the control inputs sent by the leader robot. The leader robot transmitted its control inputs to the follower using the Bluetooth piconet profile.

The posture stabilization controllers using smooth time-varying, polar coordinates and dynamic feedback controller were simulated for the leader robot. For trajectory tracking, the reference trajectory was generated using the feedforward command controller. The multi agent nonholonomic robotic system was modeled using MATLAB/Simulink and the feedback strategies were simulated for a given set of reference trajectories. Based on the simulation results for the various trajectories, the following conclusions are made:

- For the leader robot, the full state linearized controller via dynamic feedback minimizes the mean of error more rapidly than the other feedback strategies.
- The full state linearized dynamic feedback controller for the leader robot achieves posture stabilization.
- The feedback strategies designed using cascaded systems theory and using linearization of corresponding error model fail to track the trajectory if the leader robot's starting point and the trajectory starting point is not the same (circular shaped trajectory).

- The feedback strategy designed using approximated linearization results in a time-varying controller. Hence, asymptotic stability is not guaranteed.
- For the follower robot, the input-output feedback linearized controllers minimize the error between the actual and the desired trajectory.
- If the formation structure is changed dynamically at run-time, the input-output linearized feedback controllers minimize the effect of disturbances and errors.

In summary, the feedback linearized techniques for multi agent nonholonomic robots can more rapidly minimize the error for trajectory tracking and achieve posture stabilization. For a given feasible trajectory, the full state feedback linearized strategy for the leader robot and input-output feedback linearized strategies for the follower robots are found to be more efficient in stabilizing the system.

For future work, the following work can be considered.

- In this chapter, the kinematic model of the multi agent nonholonomic robots has been considered. However, for massive robots and at high speeds, the nonholonomic constraint may not be realistic. It may happen that the robots wheels may slip due to high speed. Hence, the robots dynamics are necessary to be modeled.
- Current implementation of Bluetooth piconet profile does not support roaming protocol; hence the leadership in the formation is always static. To make the leadership more dynamic, a roaming protocol for Bluetooth can be designed.
- The leader and the follower robots are observable. Based on feedback linearized control strategies, observer based feedback laws can be designed for the leader-follower formation.

9. Acknowledgements

The authors would like to thank the Malaysian Ministry of Science, Technology and Innovation for funding this research project through IRPA grant 04-99-02-0003-EA001.

10. References:

Aicardi, M., Casalino G., Balestrino, A. and Bicchi, A. (1995). Close loop steering of unicycle like vehicles via Lyapunov techniques, *IEEE Robotics and Automation Magazine*, pp. 27- 35, vol. 2, issue 1.

Balch, T. and Arkin, R. C., (1998). Behavior-based formation control for multi-robots teams, *IEEE Transactions on Robotics and Automation*, pp. 926-939, vol. 14, no. 6.

Bichhi A., and L. Pallottino, L., (2000). On optimal cooperative conflict resolution for air traffic management systems, *IEEE Transactions on Intelligent Transportations Systems*, vol. 1, no. 4.

Clark, C. M. (2004). *Dynamic Robots Network: A Coordination Platform for Multi-robot Systems, PhD Thesis*, Department of Aeronautics and Astronautics, Stanford University.

Das, A. V. et. al (2002), A vision-based formation control framework, *IEEE Transactions on Robotics and Automation,* pp. 813-825, vol. 18, no. 5.

Desai, J. P. (1998). *Motion Planning and Control of Cooperative Robotic Systems*, *PhD Thesis*, Mechanical Engineering and Applied Mechanics, University of Pennsylvania.

Desai, J. P., Ostrowski, J. and Kumar, V. (1998). Controlling formations of multiple mobile robots, *IEEE International Conference on Robotics & Automation*, Belgium.

Ferber J., (1999). *Multi Agent Systems: An Introduction to Distributed Artificial Intelligence*, Addison Wesley Longman, England.

FIPA Agent Communication Language Specifications, (2002) [online]. [Accessed 15 Sept. 2008]. Available from World Wide Web: <http://www.fipa.org/repository/aclspecs.html>

Kanayama, Y., Kimura, Y., Miyazaki F. and Noguchi, T. (1991). A stable tracking control method for a nonholonomic mobile robot, *IEEE International Workshop on Intelligent Robots and Systems*, pp. 1236-1241, Japan,.

Khalil, H.K. (2002). *Nonlinear Systems*, 3rd edition, Prentice Hall.

Kolmanovsky, I. and McClamroch, N. H. (1995). Developments in nonholonomic control problems, *IEEE Control Systems Magazine*, pp. 20–36, vol. 15, issue 6.

Langer, D., Rosenblatt, J. K. and Hebert, M. (1994). A behavior-based system for off-road navigation, *IEEE Transactions on Robotics and Automation*, vol. 10, no. 6.

Lefeber, E., Jakubiak, J., Tchon, K. and Nijmeijer, H. (2001). Observer based kinematic tracking controllers for a unicycle-type mobile robot, *IEEE Conference on Robotics & Automation*, May 2001, Seoul, Korea.

Luca, A. D., Oriolo, G. and Vendittelli, M. (2000). Stabilization of the unicycle via dynamic feedback linearization, *IFAC Symposium of Robot Control*, pp. 397-402.

Luca, A. D., Oriolo, G. and Vendittelli, M. (2001). *Control of Wheeled Mobile Robots: An Experimental Overview*, *Lecture Notes*, Diapartimento di Informatica e Sistemistica, Universita degli Studi di Roma, Itlay.

Morrow, R. (2002). *Bluetooth Operation and Use*, McGraw-Hill, New York.

Nise, N. S. (2004). *Control Systems Engineering*, 4th Edition 2004 John Wiley & Sons, New York.

Oriolo, G., Luca, A. D. and Vendittelli, M. (2002). WMR control via dynamic feedback linearization: design, implementation and experimental validation, *IEEE Transactions on Control Systems Technology*, vol. 10, no.6.

Parker, L. E., (1994). *Heterogeneous Multi-robot Cooperation, PhD Thesis*, Department of Electrical and Computer Engineering, Massachusetts Institute of Technology.

Rydesater, P., MATLAB Central File Exchange, [Last accessed 18th Sept, 2008], http://www.mathworks.com/matlabcentral/fileexchange/loadAuthor.do?objectType=author&objectId=483407

Slotine, J-J. E. and Li, W. (1991). *Applied Nonlinear Control*, Prentice Hall.

Tabuada, P., Pappas, G. J. and Lima, P. (2005). Motion feasibility of multi-agent formations, *IEEE Transactions on Robotics*, pp. 387-392, vol. 21.

Tan, K. H. and Lewis, M. A. (1997). Virtual structures for high-precision cooperative mobile robot control, *Autonomous Robots*, pp. 387-403, vol. 4.

Wit, C. C., Khennouf, H., Samson C. and Sordalen, O. J. (1994). Nonlinear control design for mobile robots", *Recent Trends in Mobile Robots*, , pp. 121-156, World Scientific Publisher, vol. 11.

Multiagent Systems

Edited by Salman Ahmed and Mohd Noh Karsiti

ISBN 978-3-902613-51-6
Hard cover, 426 pages
Publisher I-Tech Education and Publishing
Published online 01, January, 2009
Published in print edition January, 2009

Multi agent systems involve a team of agents working together socially to accomplish a task. An agent can be social in many ways. One is when an agent helps others in solving complex problems. The field of multi agent systems investigates the process underlying distributed problem solving and designs some protocols and mechanisms involved in this process. This book presents an overview of some of the research issues in the field of multi agents. It is a presentation of a combination of different research issues which are pursued by researchers in the domain of multi agent systems as they are one of the best ways to understand and model human societies and behaviours. In fact, such systems are the systems of the future.

INTECH
open science | open minds

InTech Europe
University Campus STeP Ri
Slavka Krautzeka 83/A
51000 Rijeka, Croatia
Phone: +385 (51) 770 447
Fax: +385 (51) 686 166
www.intechopen.com

InTech China
Unit 405, Office Block, Hotel Equatorial Shanghai
No.65, Yan An Road (West), Shanghai, 200040, China
中国上海市延安西路65号上海国际贵都大饭店办公楼405单元
Phone: +86-21-62489820
Fax: +86-21-62489821